



Evolution of the uranium concentration in dissolution experiments with Cr-(Pu) doped UO_2 in reducing conditions at SCK CEN

Christelle Cachoir¹ · Thierry Mennecart¹ · Karel Lemmens¹

Received: 15 December 2020 / Accepted: 3 February 2021 / Published online: 18 March 2021
© The Author(s) 2021

Abstract

Cr-doped UO_2 -based model materials were prepared at SCK CEN, mimicking modern LWR fuels, to understand the influence of Cr doping on the spent fuel dissolution behaviour in geological repository conditions. Tests were carried out with four model materials: depleted UO_2 , Cr-doped depleted UO_2 , Pu-doped UO_2 and Pu-Cr-doped UO_2 . Static dissolution experiments have been performed up to 4 months in autoclaves under 10 bar H_2 pressure with a Pt/Pd catalyst in media at pH 13.5 and at pH 9. The Cr-doping appeared to reduce the U concentrations by a factor 6 at pH 13.5, but it had no or not much effect at pH 9.

Introduction

In recent years, doped nuclear fuels have been developed with the objective of reducing the quantity of fuel used per energy output in operating i.e. Gd doping to control excess fuel reactivity without control rod, and more recently Cr (+ Al) doping to minimize fission gas release thanks to the resulting larger grain size. The addition of dopants in the UO_2 matrix can modify the stoichiometry of the initial UO_2 fluorite structure, the density of the UO_2 matrix, and the size of the UO_2 grains [1, 2]. These physical changes affect not only the fuel behaviour during operation [2], but could also impact the spent fuel behaviour in a final repository [3, 4]. While the dissolution behaviour of standard spent fuel in repository conditions has reached a good level of comprehension [5, 6], it is not clear if these doped fuels will behave similarly. Hence, dissolution experiments with simplified UO_2 -based model materials have been carried out within the EU-DisCo project [7]. The experiments by SCK CEN focused on Cr-doped materials, with a larger grain size than standard fuels. To study the effect of alpha activity, Pu was added as well to the UO_2 , yielding an alpha dose representative of 10,000 years old spent fuel. UO_2 batches without Cr or Pu were tested for comparison. The tests were

done in a Young Cementitious Water at pH 13.5 and bicarbonate solution at pH 9.

Experimental

Materials

The UO_2 model materials were synthesised at SCK CEN in collaboration with FZ Juelich. The production method was optimized to reach $95 \pm 1\%$ of the theoretical UO_2 density and to approach a grain size of 50 μm and a more or less homogeneous Cr distribution within the UO_2 matrix. Homogeneous α -doping was obtained by co-dissolving in nitric acid a given amount of certified depleted UO_2 and a smaller amount of an existing batch of $^{238}\text{Pu}/^{233}\text{U}$ doped UO_2 powder [8] to reach α -doping level representative for a fuel age of 10,000 years ($\sim 18 \text{ MBq/g } \text{UO}_2$). The solution of (Pu doped) uranyl nitrate is then precipitated as ADU ($(\text{NH}_4)_2\text{U}_2\text{O}_7$), oxidised to U_3O_8 and finally reduced to UO_2 . A blend of 80% (Pu-) UO_2 / 20% U_3O_8 is then mixed with 1600 μg Cr_2O_3 powder per g UO_2 and 0.3 wt% zinc stearate (lubricant) [9]. Pellets are pressed around 550 MPa and sintered at -410 kJ/mol at 1700 °C for 8 to 24 h in a flowing gas mixture of Ar- 4% H_2 and Ar- 0.5% O_2 .

Four model materials were achieved (Table 1): depleted UO_2 (UO_2), Cr-doped depleted UO_2 (Cr- UO_2), Pu-doped UO_2 (Pu- UO_2) and Pu-Cr-doped UO_2 (Pu-Cr- UO_2). Although the Cr doping resulted in an increase of the average grain size of both Cr- UO_2 and Pu-Cr- UO_2 (Fig. 1), a

✉ Christelle Cachoir
ccachoir@sckcen.be

¹ SCK CEN, Waste and Disposal Unit, Mol, Belgium

Table 1 Specifications of the UO₂ based materials

Type of model material	UO ₂	Cr-UO ₂	Pu-UO ₂	Cr-UO ₂
Pellet (ϕ/ h-mm)	5.82/ 7.12	5.79/ 6.45	5.85/ 2.85	5.85/ 2.85
TD % ^a	96 ± 1	95 ± 1	93.8 ± 1	93.5 ± 1
Cr ₂ O ₃ added (μg.g ⁻¹)	–	1600	–	1600
Average grain size (μm) ^b	10	38–48	14.5	26
Grain size periphery (μm) ^b	10	10	10	10

^aTD% is the percentage of the theoretical UO₂ density, measured by immersion technique.

^bGrain size analyses were performed according to the line intercept method (ASTM Standard E112-13- [11]) with grain boundaries revealed by etching with HF+CrO₃ (UO₂, Cr-UO₂ samples) or by scanning electron microscopy with backscattered electron (α-doped samples).

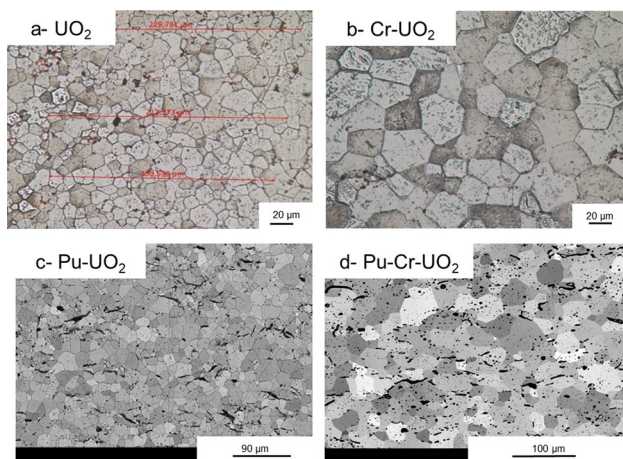


Fig. 1 Average grain size of UO₂ based materials **a** 10 μm for UO₂, **b** 38–48 μm for Cr-UO₂, **c** 14.5 μm for Pu-UO₂, **d** 26 μm for Pu-Cr-UO₂

50-μm band of grains with diameter around 10 μm is present at the pellet periphery, as a result of Cr evaporation during the sintering process [10]. All materials exhibit a rather homogeneous intergranular porosity (Fig. 1). The Pu-Cr-UO₂ pellets (Fig. 1d) also showed many intragranular pores, which possibly explains the lower density compared to the other model systems. The specifications of the model materials are given in Table 1.

Set-up and procedure

Static dissolution experiments were carried out with the four model materials, added as pellets: ‘inactive tests’ with UO₂ and Cr-UO₂ and ‘active tests’ with Pu-UO₂ and Pu-Cr-UO₂. The tests were done in two leaching solutions (Table 2): Young Cementitious Water at pH 13.5 (YCWCa) and in bicarbonate solution at pH 9 [12]. All experiments

Table 2 Measured initial composition of the leaching solutions at pH 13.5 and pH 9

mol.L ⁻¹	Medium pH 13.5	Medium pH 9
Na	1.28 × 10 ⁻¹	2.07 × 10 ⁻²
K ^a	3.67 × 10 ⁻¹	2.33 × 10 ⁻⁵
Ca ^a	4.43 × 10 ⁻⁴	5.00 × 10 ⁻⁶
C	5.08 × 10 ⁻⁴	9.83 × 10 ⁻⁴
SO ₄ ^{2-a}	1.86 × 10 ⁻³	5.21 × 10 ⁻⁶
Si ^a	4.32 × 10 ⁻⁵	3.71 × 10 ⁻⁵
Cl	< 8.45 × 10 ⁻⁶	1.81 × 10 ⁻²
U ^a	< 8.40 × 10 ⁻¹⁰	< 8.40 × 10 ⁻¹⁰
Cr ^a	4.93 × 10 ⁻⁸	< 1.35 × 10 ⁻⁸
Zn ^a	2.29 × 10 ⁻⁷	1.17 × 10 ⁻⁷
Measured pH	13.6 ± 0.2	9.1 ± 0.2

^aThese elements are not part of the composition, but they are measured either to compare both solutions (K, SO₄²⁻, Si) or to define the background concentration (U, Cr, Zn)

were performed in autoclaves with 10 bar H₂ gas in an Ar glove box (pO₂ below 10 ppm and pCO₂ below the detection limits) and at 20–25 °C. A Pt/Pd catalyst was placed in the headspace of the autoclaves (not immersed in the solution) to scavenge the traces of atmospheric oxygen inside the autoclaves by reaction with the H₂ gas, without perturbation of the radiolytical reactions in the solution (Fig. 2a). No other reducing agents were added to the solution, as preliminary tests demonstrated little effect [12].

The set-up consists of stainless steel autoclaves with a PEEK insert of 50 ml (Fig. 2b and c). The cover of the autoclaves is equipped with two outlet valves; one short inlet tube stopping immediately under the cover for gas inlet and one longer outlet tube near the bottom of the solution for the sampling of the solution. Gas pressure (H₂) is monitored during the experiment by a manometer. Each autoclave is filled with 30 ml of solution and one pellet of (doped) UO₂ (Table 1), corresponding to an initial ratio of UO₂ surface area to solution volume (SA/V) of 6 m⁻¹ and 3 m⁻¹ for the inactive and the active experiments, respectively. Prior to the leaching test, the pellets were washed in 30 ml of 0.01 M NaCl in a PE bottle for a period of three to five weeks with a daily renewal the first week and a weekly renewal for the weeks thereafter [12]. One week before the end of the washing step the autoclaves were filled with 30 ml of the leaching solution (Table 2) in presence of the Pd/Pt catalyst with 5 bar H₂ pressure. When the U concentration within the washing solution stayed in the range of the U(IV) solubility (10^{-8.5 ± 1} M) [13], the pellets were transferred from the PE bottle to the autoclaves and the leaching experiment was started for a period up to 4 months. After 1, 3, 10, 30 (35), 72 and 155 days, an aliquot of 2 ml was sampled without

replenishment of solution and the autoclave was pressurised again up to 10 bar H_2 pressure. For the Pu doped samples, the duration of 155 days was not yet reached when this paper was written.

The total U concentrations (without filtration) were measured during the washing and the leaching period while the soluble U concentrations (ultrafiltration < 3.5 nm) were only determined at pH 9 or pH 13.5. ^{238}U was measured by ICP-MS for the inactive experiments while ^{233}U and ^{238}Pu were measured by alpha-spectrometry for the active experiments. pH of the leachate was monitored over time and Cr and Zn (lubricant) concentrations were also quantified by ICP-MS. In this paper, we focus only on the evolution of the U concentrations.

Fig. 2 Experimental set-up **a** inside cell, **b** schematic drawing and **c** autoclaves under 10 bar H_2 pressure

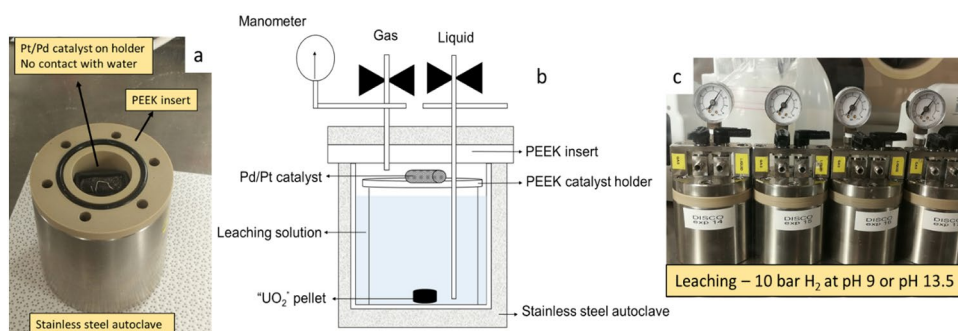


Fig. 3 Total U concentrations as a function of time with 10 bar H_2 **a** at pH 13.5 for inactive experiments (red symbols) and active experiments (green symbols); **b** at pH 9 for inactive experiments (blue symbols—empty symbol \leq detection limit) and active experiments (yellow symbols). On both graphs, the black dotted lines represent the U(IV) solubility range [13]

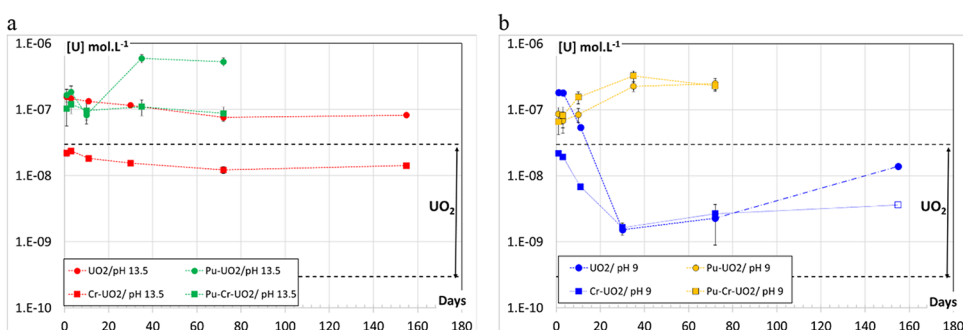


Table 3 U concentration ($mol.L^{-1}$) as function of time in the experiments with UO_2 and $Cr-UO_2$ pellets at pH 13.5 and at pH 9

Days	pH 13.5				pH 9			
	UO_2		$Cr-UO_2$		UO_2		$Cr-UO_2$	
	$[U]_T$	$[U]_s$	$[U]_T$	$[U]_s$	$[U]_T$	$[U]_s$	$[U]_T$	$[U]_s$
	$\times 10^{-8} mol.L^{-1}$				$\times 10^{-8} mol.L^{-1}$			
1	15.6 ± 1.6	15.3 ± 1.6	2.2 ± 0.2	2.2 ± 0.2	18.4 ± 1.9	16.0 ± 1.6	2.2 ± 0.2	2.2 ± 0.2
3	14.7 ± 1.5	14.2 ± 1.4	2.4 ± 0.2	2.3 ± 0.2	18.1 ± 1.8	16.3 ± 1.7	1.9 ± 1.9	1.7 ± 0.2
11	13.4 ± 1.3	11.9 ± 1.2	1.8 ± 0.2	1.7 ± 0.2	5.4 ± 0.6	5.2 ± 0.5	0.7 ± 0.07	0.6 ± 0.06
30	11.6 ± 1.2	11.0 ± 1.1	1.6 ± 0.2	1.5 ± 0.2	0.2 ± 0.5	0.1 ± 0.4	0.2 ± 0.05	0.1 ± 0.04
72	7.7 ± 0.8	6.8 ± 0.7	1.2 ± 0.1	1.0 ± 0.1	0.2 ± 0.03	< 0.06	0.3 ± 0.03	< 0.06
155	8.2 ± 0.8	4.3 ± 0.4	1.4 ± 0.1	0.5 ± 0.3	1.4 ± 0.1	< 0.4	< 0.4	< 0.4

$[U]_T$ = not filtered U concentration and $[U]_s$ = ultrafiltered U concentration (< 3.5 nm)

Results and discussion

Figure 3 shows the total U concentration as a function of time for the different model materials at pH 13.5 (Fig. 3a) and at pH 9 (Fig. 3b). Tables 3 and 4 give the measured total and soluble U concentrations as a function of time for the inactive and active experiments, respectively.

pH 13.5

For the inactive experiments (Fig. 3a—red symbols) after a high initial U release, up to 1.6×10^{-7} for UO_2 and $2.2 \times 10^{-8} mol.L^{-1}$ for $Cr-UO_2$, the U concentration slightly decreased. After 155 days, the U concentration stabilised

Table 4 U concentration (mol.L⁻¹) as function of time in the experiments with Pu-UO₂ and Pu-Cr-UO₂ pellets at pH 13.5 and in at pH 9

Days	pH 13.5				pH 9			
	Pu-UO ₂		Pu-Cr-UO ₂		Pu-UO ₂		Pu-Cr-UO ₂	
	[U] _T	[U] _s	[U] _T	[U] _s	[U] _T	[U] _s	[U] _T	[U] _s
	× 10 ⁻⁸ mol.L ⁻¹				× 10 ⁻⁸ mol.L ⁻¹			
1	16.6 ± 3.6	13.8 ± 3.9	10.3 ± 4.7	8.4 ± 3	8.6 ± 2.3	8.8 ± 2.9	6.7 ± 2.3	8.8 ± 2.9
3	18.5 ± 4.5	8.9 ± 3	12.1 ± 3.4	11.4 ± 3	6.9 ± 2.4	5.4 ± 2	8.2 ± 2.9	5.4 ± 2.5
11	8.3 ± 2.2	10.2 ± 2.4	9.7 ± 2.6	8.4 ± 2.5	8.4 ± 2	11.7 ± 2.9	15.5 ± 3.2	18.7 ± 3.9
35	59.5 ± 8.3	57.4 ± 8.4	11.1 ± 3	11.2 ± 2.5	22.7 ± 3.8	20.2 ± 3.9	32.7 ± 6.2	29.9 ± 5.4
72	53.1 ± 7.8	53.4 ± 8.4	8.8 ± 2.2	9.9 ± 3	24.9 ± 5	23.6 ± 4.9	23 ± 4	25 ± 4.9

[U]_T = not filtered U concentration and [U]_s = ultrafiltered U concentration (< 3.5 nm)

around 8.2×10^{-8} for UO₂ and 1.4×10^{-8} mol.L⁻¹ for Cr-UO₂. The presence of Cr thus reduced by a factor 6–7 the U concentration over the entire test duration.

For the active experiments (Fig. 3a-green symbols) a high initial U release of 1.7×10^{-7} for Pu-UO₂ and 1.0×10^{-7} mol.L⁻¹ for Pu-Cr-UO₂ is also observed with no clear influence of Cr up to 10 days. Afterwards, while the U concentration remained around 1.0×10^{-7} mol.L⁻¹ for Pu-Cr-UO₂, the U concentration for Pu-UO₂ increased. After 35 days, the U concentration is 6 times higher than for the Pu-Cr-UO₂, and remains stable close to 5.3×10^{-7} mol.L⁻¹ (Fig. 3a- green symbols). This suggests that, at pH 13.5, the Cr doping lowers the U concentration also in presence of alpha field.

In most cases, the U concentration in the ultrafiltered samples represents more than 90% of the total U concentration (Tables 3 and 4), the difference corresponding to the uncertainty of measurement techniques. However the U-colloids (= difference between total and soluble U concentrations) are increasing after 155 days in the UO₂ system without α-field, possibly as precursors of a U-phase formation. Further analyses and data modelling are needed to support this hypothesis.

pH 9

For the inactive experiments, a high initial U release of 1.8×10^{-7} for UO₂ and 2.2×10^{-8} mol.L⁻¹ for Cr-UO₂ was measured (Fig. 3b blue-symbols). Then, the U concentration considerably decreased with time to stabilize after 30 days around 2×10^{-9} mol.L⁻¹ for both systems. This suggests a possible control of the U in solution by UO₂. The higher ratio of colloidal U/total U (Table 3) supports the possible over-saturation with a U secondary phase, but the concentration of colloidal U remains small (about 10^{-9} M). During the first 10 days of leaching, the presence of Cr seems to reduce the U release, similarly as at pH 13.5 (Fig. 3a- blue symbols), but this effect disappears with time. After 72 and 155 days the U concentration showed a slight increase, more for UO₂ than for Cr-UO₂. This suggests

again a reducing effect of the Cr. As the experiments were stopped after 155 days, we cannot verify if this trend continues afterwards.

For the active experiments, the initial U concentration is high again ($9-7 \times 10^{-8}$ mol.L⁻¹- Fig. 3b- yellow symbols). After this initial release, the U concentration slightly increases and stabilises around 2.5×10^{-7} mol.L⁻¹ after 35 days (Fig. 3b-yellow symbols). There is no pronounced Cr effect. The presence of U colloids in active experiments at pH 9 is also rather limited and remains within the uncertainties of the alpha-spectrometry (Table 4).

In all systems, the high initial U release suggests the dissolution of a slightly oxidised UO_{2+x} layer in spite of the washing. Possibly some oxidation of the pellet occurred during the transfer from the PE bottle used for the washing to the autoclave, even if the oxygen concentration in the glove box is < 10 ppm. This initial release is not affected by pH, complexing agent (OH⁻ or CO₃²⁻) or alpha field. On the other hand, we can clearly distinguish a lowering effect of Cr on the initial U(VI) release in absence of alpha field at both pHs. A similar reducing Cr effect appears slightly delayed at pH 13.5 in presence of alpha field, but it is not present at pH 9. These results suggest that at high pH, Cr makes the UO₂ surface more resistant against oxidation, or prevents the release of U(VI) from the surface. For the inactive tests, the measured U concentrations are higher at pH 13.5 than at pH 9 (Fig. 3-red and blue symbols). These concentrations remain nevertheless within the UO₂ solubility range [13], except for UO₂ at pH 13.5 showing a higher U concentration [14, 15]. These observations reveal a favoured complexation of U(VI) from the remaining oxidised layer by the hydroxyl ions at high pH compared to hydrogeno-carbonate ions at pH 9.

In presence of an α-field, the measured U concentrations are always higher than the UO₂ solubility range. This is caused by radiolytical oxidation in spite of the H₂ gas. For Pu-Cr-UO₂ at pH 13.5, the concentrations stabilize immediately after the initial release around 1×10^{-7} mol.L⁻¹, while for Pu-UO₂ a renewed release occurs between

10 and 35 days to reach a U concentration of 5×10^{-7} mol.L⁻¹. This suggests again a stabilising effect of the Cr at high pH. A renewed release is observed also for Pu-UO₂ and Pu-Cr-UO₂ at pH 9, reaching concentrations of about 2.5×10^{-7} mol.L⁻¹. At this lower pH, the Cr has no stabilising effect. After 35 days, no further increase of the U concentration is detected. This suggests that on the short term the dissolved H₂ cannot prevent radiolytical UO₂ oxidation or U(VI) dissolution, or reduce back U(VI) in solution, but after a period of renewed oxidation or release, it could become effective. Another explanation of the flattening of the concentration after 35 days could be the control of U in solution by a U-phase. Such flattening effect was already observed in tests with Pu-doped UO₂ without Cr with a similar alpha activity although no H₂ gas was present [16]. At pH 13.5, the Cr doping could increase the H₂ effect, but whatever the experiment this H₂ effect was not effective enough to reach U concentrations at the level of the UO₂ solubility range.

In spite of the fact that the outermost layer of the Cr-doped pellets has a relatively small grain size and Cr concentration, we thus observe an effect of the Cr doping in certain conditions. Several hypotheses can be proposed to explain these observations: a redox effect of the chromium in solid or in solution, enhanced catalytic properties of the UO₂ surface by the presence of Cr, increasing the reduction of oxidising species by H₂, or formation of a phase at the UO₂ surface blocking the further dissolution. Based on our current results, none of these hypotheses can be favoured, but modelling calculations or surface analysis are considered to support the data interpretation. In parallel, these experiments will be compared to similar experiments done at VTT-Technical Research Centre of Finland with the same materials, but using metallic iron to control the redox conditions in place of hydrogen.

Conclusions

Static leaching experiments were performed with Pu and Cr doped UO₂ in a cementitious water with pH 13.5 and a bicarbonate solution with pH 9 in autoclaves under 10 bar H₂ pressure, and compared with undoped analogues. The Cr-doping appeared to reduce the U concentrations in solution for UO₂ with and without Pu at pH 13.5, but not or much less at pH 9. For both leaching media, the effect of dissolved H₂ was not sufficient to prevent the short term radiolytical oxidation/dissolution, or to reduce oxidised U(VI) in solution. All uranium concentrations were higher than the solubility of UO₂ in reducing conditions, but the stabilization of the uranium concentrations for the Pu doped UO₂ with time could still be ascribed to the presence of H₂ or to the solution saturation by a U-phase. The

Cr doping could favour the H₂ effect at pH 13.5. Surface analysis of the leached surface, modelling calculations and other method to control the redox conditions are ongoing to explain the observed Cr effects.

Acknowledgements The research leading to these results has received funding from the European Commission Horizon 2020 Research and Training Programme of the European Atomic Energy Community (EURATOM) (H2020-NFRP-2016-2017-1) under Grant Agreement n° 755443 (DisCo project).

Data availability All data presented herein are available upon request.

Compliance with ethical standards

Conflict of interest The authors declare no competing interests.

Open Access This article is licensed under a Creative Commons Attribution 4.0 International License, which permits use, sharing, adaptation, distribution and reproduction in any medium or format, as long as you give appropriate credit to the original author(s) and the source, provide a link to the Creative Commons licence, and indicate if changes were made. The images or other third party material in this article are included in the article's Creative Commons licence, unless indicated otherwise in a credit line to the material. If material is not included in the article's Creative Commons licence and your intended use is not permitted by statutory regulation or exceeds the permitted use, you will need to obtain permission directly from the copyright holder. To view a copy of this licence, visit <http://creativecommons.org/licenses/by/4.0/>.

References

1. A. Massih, Effect of additives on uranium dioxide fuel behaviour. Swedish Radiation Safety Authority 2014-21 ISSN 2000-0456, Sweden (2014).
2. N. Liu, J. Kim, J. Lee, Y.S. Youn, J.G. Kim, J.Y. Kim, J.J. Noël, D.W. Shoesmith, *Electrochim. Acta* **247**, 496 (2017)
3. D. Horlait, N. Clavier, S. Szenknect, N. Dacheux, V. Dubois, *Inorg. Chem.* **51**, 3868 (2012)
4. M. Razdan, M. Trummer, D. Zagidulin, M. Jonsson, D.W. Shoesmith, *Electrochim. Acta* **130**, 29 (2014)
5. R. Ewing, *Nat. Mater.* **14**, 252 (2015)
6. D. Shoesmith, Uranium: cradle to grave. In: Burns, Sigmon, eds., Mineralogical Association of Canada Short Course Series vol. 43, 337 (2013)
7. DISCO: Modern spent fuel DISsolution and chemistry in failed COntainer conditions (2016). <https://www.disco-h2020.eu>. Accessed 08 Dec 2020
8. C. Cachoir, K. Lemmens in Scientific Basis for Nuclear Waste Management edited by Oversby and Werme (Mat. Res. Soc. Symp. Proc 807, Kalmar, Sweden 2003) pp 59–64
9. R. Delville, Presented at the 30th Spent Fuel Workshop in Ghent Belgium 2019 (unpublished)
10. T. Cardinaels, K. Govers, B. Vos, S. Van den Berghe, M. Verwerft, L. de Tollenaere, G. Maier, C. Delafoy, *J. Nucl. Mater.* **424**, 252 (2012)
11. ASTM E112-13: Standard Tests Methods for determining average grain size, International, West Conshohocken, PA, ASTM 2013. <https://www.astm.org>. Accessed 08 Dec 2020
12. D. Bosbach, C. Cachoir, E. Myllykylä, C. Jegou, J. Cobos, I. Farnan, C. Corkhill. Deliverable D4.1 of the European DisCo

- project (2019). <https://www.disco-h2020.eu/Home/Deliverables>. Accessed 08 Dec 2020
13. V. Neck, J.I. Kim, *Radiochim. Acta* **89**(1), 1 (2001)
 14. T. Mennecart, C. Cacho, K. Lemmens, J. *Radioanal. Nucl. Chem* **304**(1), 61 (2015)
 15. C. Cacho, S. Salah, T. Mennecart, K. Lemmens, *Proc. Chem.* **21**, 306 (2016)
 16. C. Cacho, T. Mennecart, Level 5 report “Spent fuel Dissolution in Supercontainer conditions” RP.W&D.0060: Programme 2009–2014. SCK CEN report ER-231 (2016)